Electrical Power and Energy Systems 153 (2023) 109380

Contents lists available at ScienceDirect

International Journal of Electrical Power and Energy Systems

journal homepage: www.elsevier.com/locate/ijepes

Identifying suitable DC system models for an independent design of VSC controllers in MTDC grids

Fatemeh Ahmadloo *, Sahar Pirooz Azad

Department of Electrical and Computer Engineering, University of Waterloo, Waterloo, N2L 3G1, Ontario, Canada

ARTICLE INFO

Keywords:
AC-DC power converter
Control systems
HVDC transmission
Stability

ABSTRACT

In AC-multi-terminal DC (MTDC) systems, if converter controllers are designed individually, the interactive system modes stemming from the dynamic couplings among the converters and the DC system components may result in the instability of the interconnected system (INTSYS). This paper presents a comparative system-level study to determine the suitable models for an individual design of converter controllers to prevent INTSYS instability. The goal is to identify suitable individual system (INDSYS) models that do not contain the internal dynamics of adjacent converters and only include the coupling dynamics corresponding to the interactive system modes among the converters. The use of these models for control design will result in the dynamic response of the INTSYS being close to that of the INDSYS models. Furthermore, such models can ensure INTSYS stability when converter controllers are designed individually without requiring the complete model of the INTSYS or internal dynamics of the adjacent converters. Both the master–slave and the droop control modes of operation are analyzed, and specific INDSYS models among those available in the literature are recommended for each operation mode. Time-domain simulations in PSCAD validate the accuracy of the INDSYS models. Furthermore, eigenvalue analysis along with the participation factor and sensitivity analyses for a large set of control parameters are employed to evaluate the efficacy of the recommended models.

1. Introduction

The growing need for affordable and clean energy has resulted in various alterations in power grids. One example is the formation of multi-terminal direct current (MTDC) systems, which enables power transmission over long distances and the integration of renewable energy sources within the grid. In an MTDC system, the direct current (DC) system is connected to the alternating current (AC) system via several voltage-sourced converters (VSCs) [1].

The trend toward an increased number of converters in MTDC systems has turned AC-MTDC system stability into a compelling topic that has been studied in several papers [2–10]. As shown in [2], in an MTDC system, there might exist several interactive system modes that are associated with more than one converter and with DC transmission lines. These interactive modes are different from the local modes that originate from one single converter or only the DC system. These interactive modes stem from the dynamic interactions among the converter stations and the DC system components that are not considered in the control design of individual converters [2,8]. Due to these interactive modes, the connection of converters to a shared DC system may result in poorly-damped or unstable modes as the eigenvalue locus of the interconnected AC-MTDC system may differ from that of the individual converters' models for which the controllers are designed [3].

Three approaches have been proposed in the literature to address the undesired impact of interactive system modes on AC-MTDC system performance. The first approach is to modify the control system of the converters based on the interconnected system modes, as suggested in [2]. This process requires the entire AC-MTDC system model and might be iterative, costly, and time-consuming, specifically if the number of converters and thus the number of state and controlled variables is large. The second approach to prevent poorly damped or oscillatory interactive system modes is to employ supplementary controllers for each converter station, obtained through an impedance matching process by solving an optimization problem [11,12]. The drawbacks of such an approach are associated with the selection of appropriate weighting functions and the cost of adding an additional controller to each converter. Simultaneous design of the controllers for all the converter stations, considering the entire AC-MTDC system dynamics, is the third approach that is used in [13] to mitigate the poorly damped modes and stabilize the system through solving an optimization problem. However, as the size of an MTDC system increases, achieving a simultaneous control design for all the converter stations may be challenging.

* Corresponding author.
E-mail address: fahmadlo@uwaterloo.ca (F. Ahmadloo).

https://doi.org/10.1016/j.ijepes.2023.109380
Received 8 February 2023; Received in revised form 15 May 2023; Accepted 13 July 2023
Available online 4 August 2023

This paper proposes another approach to prevent interconnected AC-MTDC system instability by involving the interactive modes in the individual design of converter controllers. To do so, suitable system models, which do not rely on the full dynamic model of the AC-MTDC system, but include the interactive system modes, are required for converters' controller design. However, most of the system models employed in stability and interaction analyses of AC-MTDC systems are the current source based models, where the adjacent converters are modeled as current sources and the dynamics of the DC system are not considered [2,3,5,7,8,11,14–18]. Although [19] includes the DC system dynamics in the developed model, it includes the impact of other converters connected to the DC system in the impedance connected to the DC side and, thus, relies on the full dynamics of the system. In [4,9,20–22], the components included in the model of each converter are not clearly described, and it is not evident whether the couplings among the converters are considered in the control design. In the interconnected system (INTSYS) model in [2,23,24], the converters are modeled by their equivalent droop or current source model, but the inclusion of the interactive modes into the model of individual converters is not discussed.

In this paper, using available core models in the literature, a comparative study has been done and suitable individual system models are selected to enable designing converter controllers independent of those of the adjacent converters. These individual system models will be referred to as INDSYS in the rest of the paper. Proper selection of INDSYS models by including the dynamics of certain components of the converters' DC side would lead to a close matching between the dynamics of the interconnected AC-MTDC system and INDSYS models. This paper does not propose a new controller or an MTDC system model and only focuses on how the DC system including the DC lines and adjacent converters should be modeled when the converter controllers are designed individually such that the INTSYS stability is ensured when the individually designed controllers are employed.

The objective of this paper is to select suitable INDSYS models, which are primarily used for the control design of each converter, such that the following specifications are met: (1) the superimposed eigenvalue locus of these models is close to the eigenvalue locus of the INTSYS, and (2) these models do not include the internal dynamics of adjacent converters. The first specification guarantees a close matching between the dynamic response of the converters operating individually and when connected to other converters. The second specification enables the individual design of converter controllers without any need to access the entire INTSYS model or the internal dynamics of adjacent converters. The proposed approach of this paper simplifies the control design of large-scale INTSYSs as the control design is performed for several small subsystems rather than a single large INTSYS. Both master–slave and droop control modes are analyzed, and specific individual models are proposed for each mode. In the master–slave mode of operation and for the converter controlling the active power, only one INDSYS model is used based on an observability analysis. For the converter controlling the DC voltage, two models, which differ from each other in terms of DC line and adjacent converter dynamics, are studied, and the most suitable INDSYS model is selected. For droop control mode, an INDSYS model that incorporates the dynamics of the DC transmission lines and the operating modes of adjacent converters is selected and is compared against the current source model. Using eigenvalue, sensitivity, and participation factor analyses, it is demonstrated that the selected INDSYS models meet the two necessary specifications that were discussed above and thus are appropriate choices for individual control design. Furthermore, the eigenvalue analysis shows that for low short circuit ratio (SCR) values, an improper choice of models for individual control design can cause unforeseen instability in the INTSYS.

2. Interconnected AC-MTDC system dynamics

Fig. 1a shows the schematic diagram of the INTSYS, which includes three VSCs connected to a shared DC system. The system includes only three VSCs (as an example of a system with a larger number of converters) to be able to consider all possible control scenarios and provide a comprehensive analysis. Each converter is connected to the AC grid; modeled by a voltage source behind an impedance; through a filter and is connected to the other converters via DC transmission lines. Because the presented study in this paper is a small-signal analysis, an RL line model including a resistor and an inductor is considered [6]. The parallel capacitors in the DC lines' model can be included in the capacitors connected to the DC terminal of the converters. Fig. 1b shows the control system of the converters in the direct quadrature (dq) rotating frame [25]. The dq indices represent the d- and q-axis components of a variable; i and v, P, Q, respectively refer to the line current at the AC side of the converter, as well as voltage, active power and reactive power at the AC terminal of the converter; and θ_{pll} indicates the reference frame angle provided by the phase-locked loop (PLL).

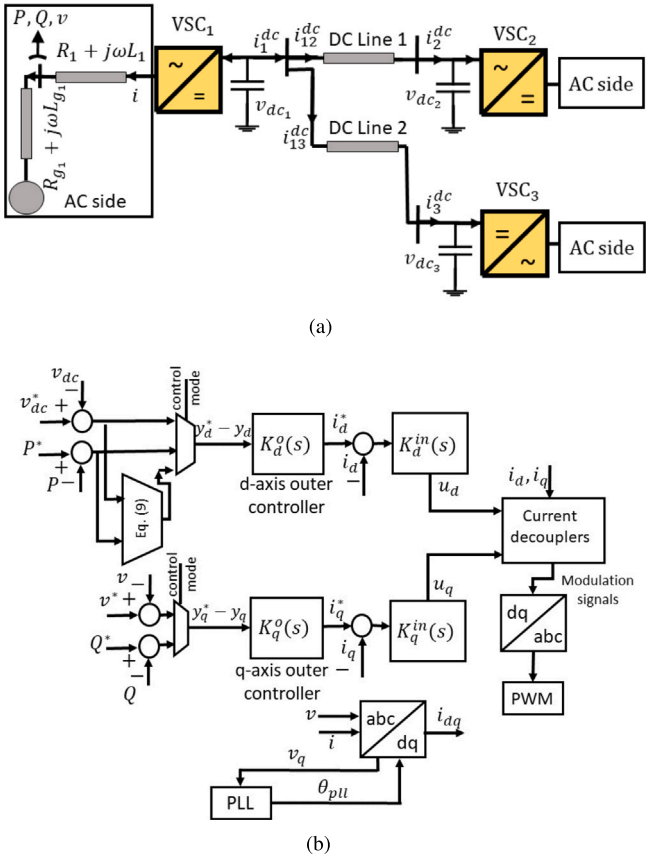

Fig. 1. (a) Single line diagram of three converters connected to a shared DC system and (b) control system of each converter.

Considering the dynamics of the dq-components of AC line currents, PLL, active and reactive power in their most general form [25], as well as the DC side dynamics, the open-loop small-signal state-space model for the INTSYS is given by

$$\dot{x} = Ax + Bu, \tag{1}$$

$$y = Cx + Du, \tag{2}$$

where $x = [x_1, x_2, x_3, i_L]^T$, $x_i = [\Delta i_d, \Delta i_q, \Delta\theta_{pll}, x_{pll}, \Delta v_{dc}]^T$; for $i \in \{1,2,3\}$ and x_{pll} represents the internal state of PLL, $i_L = [\Delta i_{12}^{dc}, \Delta i_{13}^{dc}]^T$,

$y = [\Delta y_1, \Delta y_2, \Delta y_3]^T$, $u = [\Delta u_1, \Delta u_2, \Delta u_3]^T$, and the control signal u_i is generated by the local controller of VSC$_i$ in the dq-axis frame as $u_i = [u_{d_i}, u_{q_i}]^T$ and $y_i = [y_{d_i}, y_{q_i}]^T$. For the converter in DC voltage control mode (DVCM), $y_{d_i} = v_{dc_i}$, for a converter in active power control mode (APCM), $y_{d_i} = P_i$, and for a converter in the droop control mode of operation, y_{d_i} is a combination of active power and DC voltage. y_{q_i} is the q-axis control output, which can be either AC voltage or reactive power, or a combination thereof. The fundamental equations to obtain (1)–(2) can be found in [25].

According to (1)–(2), the state variables and control inputs of all VSCs collectively impact INTSYS stability. While the inner current loops are mostly designed based on the AC filter parameters (R_1, L_1) to achieve a fast response for inner control loops [25], tuning the outer control loops for achieving the desired dynamic response depends on the coupling dynamics among the converters, which may not be included in the models used for converter controller design. Fig. 2 distinguishes between the control design and the application stages when the full dynamic model of converters is accessible or unavailable. In the control design stage, the design might be based on employing INDSYS models (Fig. 2a), which only include the necessary coupling dynamics rather than the full and detailed dynamics of adjacent converters. This approach is referred to as individual control design. In contrast, in the simultaneous design (Fig. 2b), the INTSYS model of all the converters and their detailed dynamics are required, which results in a more complex control design procedure. Ultimately, the individually or simultaneously designed controllers will be applied to the interconnected system as shown in Fig. 2c. The objective of this paper is to select suitable INDSYS models to simplify the control design and ensure interconnected system stability.

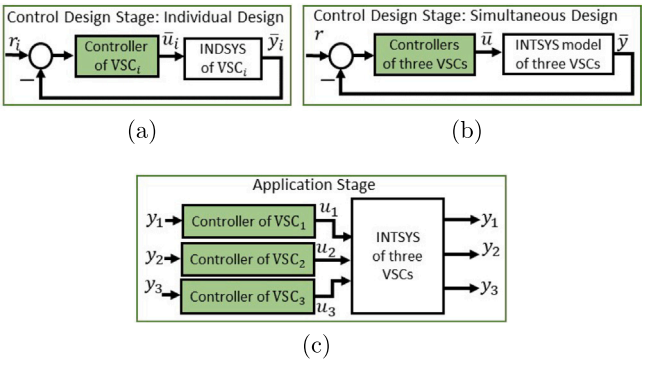

Fig. 2. Employment of the designed controllers in the INTSYS.

3. INDSYS models for converters in master-slave control mode

Various INDSYS models for converters in the master–slave control mode are presented in this section. The converters are assumed to be in the master–slave control mode, i.e., VSC$_1$ operates in DVCM, and VSC$_2$ and VSC$_3$ operate in APCM.

3.1. Operation in DVCM

Fig. 3 shows two possible INDSYS models for VSC$_1$. In the current source model (model No. 1-DVCM) in Fig. 3a, used in [3,5,7,8,11,14–18], the impact of other converters and the DC system on the DC voltage of VSC$_1$ has not been considered, and the adjacent converters operating in APCM are modeled by constant current sources. On the other hand, model No. 2-DVCM in Fig. 3b incorporates the dynamics of DC lines and the operating mode of VSC$_2$ and VSC$_3$ in the INDSYS model of VSC$_1$. It should be also mentioned that in Fig. 3b, only the operating mode of adjacent converters–not their internal and detailed

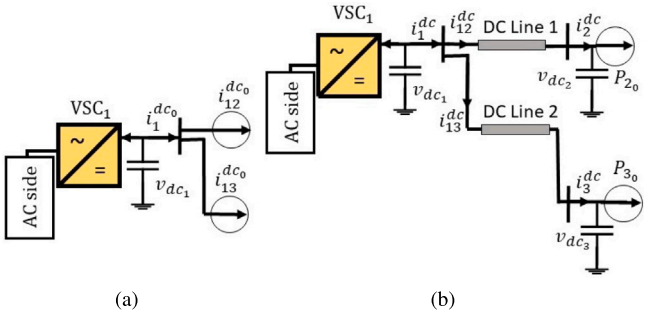

Fig. 3. INDSYS model of VSC$_1$ in DVCM: (a) model No. 1-DVCM and (b) model No. 2-DVCM.

Table 1
The DC side dynamics of the INDSYS models of VSC$_1$ in DVCM.

Model No. 1-DVCM	Model No. 2-DVCM
$C_1 \frac{dv_{dc_1}}{dt} = -\underbrace{(i_{12}^{dc_0} + i_{13}^{dc_0})}_{i_1^{dc_0}} - \frac{P_1}{v_{dc_1}}$	$C_1 \frac{dv_{dc_1}}{dt} = -\underbrace{(i_{12}^{dc} + i_{13}^{dc})}_{i_1^{dc}} - \frac{P_1}{v_{dc_1}}$
	$L_L \frac{di_{12}^{dc}}{dt} + R_L i_{12}^{dc} = v_{dc_1} - v_{dc_2}$
	$L_L \frac{di_{13}^{dc}}{dt} + R_L i_{13}^{dc} = v_{dc_1} - v_{dc_3}$
	$C_2 \frac{dv_{dc_2}}{dt} = i_{12}^{dc} - \frac{P_{2_0}}{v_{dc_2}}$
	$C_3 \frac{dv_{dc_3}}{dt} = i_{13}^{dc} - \frac{P_{3_0}}{v_{dc_3}}$
$\bar{x}_{dc} = \Delta v_{dc_1}$	$\bar{x}_{dc} = [\Delta v_{dc_1}, \Delta i_{12}^{dc}, \Delta i_{13}^{dc}, \Delta v_{dc_2}, \Delta v_{dc_3}]^T$

dynamics–are considered. Moreover, Fig. 3b shows the INDSYS model of VSC$_1$ only, which is different from [23,24] where all the converters are replaced by current sources forming the INTSYS model (not the INDSYS model).

Based on the variants shown in Fig. 3, Table 1 presents the DC side dynamics of various INDSYS models of VSC$_1$. Considering the internal dynamics of VSC$_1$ in their most general form by including the PLL and the dq-axis currents [25], as well as the DC side dynamics given in Table 1, the open-loop small-signal state-space representation of INDSYS model for VSC$_1$ will be given by

$$\dot{\bar{x}}_1 = \bar{A}_1 \bar{x}_1 + \bar{B}_1 \bar{u}_1, \tag{3}$$

$$\bar{y}_1 = \bar{C}_1 \bar{x}_1 + \bar{D}_1 \bar{u}_1, \tag{4}$$

where $\bar{x}_1 = [\bar{x}_{ac_1}, \bar{x}_{dc}]^T$, $\bar{u}_1 = [\Delta u_{d_1}, \Delta u_{q_1}]^T$, and $\bar{y}_1 = [\Delta v_{dc_1}, \Delta y_{q_1}]^T$. $\bar{x}_{dc}$ is given in Table 1 and $\bar{x}_{ac_1} = [\Delta i_d, \Delta i_q, \Delta\theta_{pll}, x_{pll}]^T$. The overbars in (3)–(4) are used to distinguish between the INDSYS and INTSYS models. In Table 1, the subscript "0" represents the operating point at which the system model is linearized. Based on Table 1, two sets of state-space models in the form of (3)–(4) are obtained for VSC$_1$ and are compared against each other in Section 5 to determine the most suitable model.

3.2. Operation in APCM

For a converter in APCM, the active power controlled at the AC terminal of the converter is described by

$$P = v_d i_d + v_q i_q, \tag{5}$$

which is independent of voltages and currents at the DC side of the converter. After linearizing (5), the state-space representation of a

converter in APCM is given by

$$\dot{\bar{x}}_k = \bar{A}_k \bar{x}_k + \bar{B}_k \bar{u}_k, \tag{6}$$

$$\bar{y}_k = \bar{C}_k \bar{x}_k + \bar{D}_k \bar{u}_k; k \in \{2,3\}, \tag{7}$$

where $\bar{y}_k = [\Delta P_k, \Delta y_{q_k}]^T$, $\bar{x}_k = [\Delta i_d, \Delta i_q, \Delta\theta_{pll}, x_{pll}, \Delta v_{dc}]^T$, and the output and state matrices have the following forms:

$$\bar{C}_k = \begin{bmatrix} \times_{2\times 4} & 0_{2\times 1} \end{bmatrix}, \bar{A}_k = \begin{bmatrix} \times & 0 & 0 & 0 & 0 \\ 0 & \times & 0 & 0 & 0 \\ \times & \times & \times & \times & 0 \\ \times & \times & \times & 0 & 0 \\ \times & \times & \times & 0 & \times \end{bmatrix}, \tag{8}$$

where $\times$ shows the non-zero elements. The zero entries in (8) are created because neither the active power in (5) nor the AC voltage/reactive power depends on the DC voltage. Based on (8), the DC voltage is an unobservable state when the converter is in APCM. Furthermore, the active power is controlled at the AC side and, thus, is not impacted by the operating mode of other converters. Therefore, it is neither necessary nor beneficial to include the dynamics of the DC terminal voltage in the state-space model of the converter in APCM. Consequently, among the two schematics shown in Fig. 4, where Fig. 4a ignores the DC side dynamics and Fig. 4b includes it, the schematic of Fig. 4a will be used as the selected INDSYS model of the converter in APCM. The state-space model of (6)–(7) is then valid with $\bar{x}_k = [\Delta i_d, \Delta i_q, \Delta\theta_{pll}, x_{pll}]^T$.

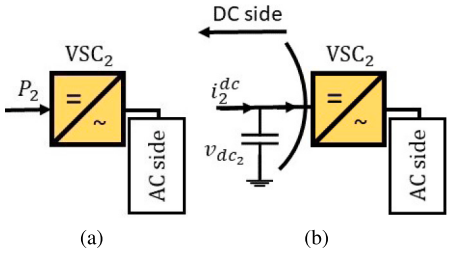

Fig. 4. INDSYS model of VSC_2 in APCM: (a) model No. 1-APCM and (b) model No. 2-APCM.

4. INDSYS model of converters in droop control mode

The droop control describes a proportional relationship between the active power and DC voltage as

$$\underbrace{P_{k,0} - P_k}_{\Delta P_k} = \left(\frac{1}{K_{dr_k}}\right)\underbrace{(v_{dc_{k,0}} - v_{dc_k})}_{\Delta v_{dc_k}}. \tag{9}$$

Based on (9), the control output in the droop control mode is a combination of DC voltage and active power ($y_{d_k} = P_k - \frac{1}{K_{dr_k}} v_{dc_k}$, or $y_{d_k} = v_{dc_k} - K_{dr_k} P_k$), in contrast to the constant DVCM or APCM. Because the DC voltage appears in the control output formulation (y_{d_k}), this converter is impacted by the adjacent converters through their DC voltages.

Fig. 5 shows two INDSYS models for VSC_2 when all converters operate in droop control mode. Fig. 5a shows the current source model (model No. 1-Droop) that has been used in the literature [11,12]. Neither the dynamics of the DC line nor the operating mode of adjacent converters are considered in this model. On the other hand, Fig. 5b shows the INDSYS model No. 2-Droop for VSC_2, in which the dynamics of DC transmission lines and the capacitor in the other converters are considered. The operating modes of adjacent converters are incorporated into this model using a voltage-dependent power source (according to (9)). This INDSYS model is different from that in [23] where the converters are replaced by current sources to form the INTSYS model.

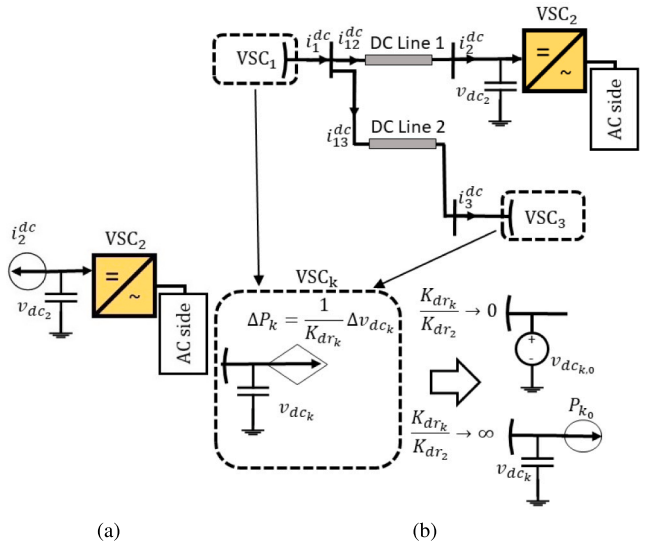

Fig. 5. INDSYS model of VSC_2 for droop mode of operation: (a) model No. 1-Droop and (b) model No. 2-Droop.

Considering Fig. 5b, if K_{dr_k} is very small compared to K_{dr_2} ($\frac{K_{dr_k}}{K_{dr_2}} \to 0$), VSC_k will experience small deviations in its DC voltage with variations in the active power. On the other hand, if K_{dr_k} is very large compared to K_{dr_2} ($\frac{K_{dr_k}}{K_{dr_2}} \to \infty$), VSC_k will experience small deviations in its active power with changes in the DC voltage. Therefore, it can be concluded that if $\frac{K_{dr_k}}{K_{dr_2}}$ is very small, VSC_k can be considered as a voltage source in the INDSYS model of VSC_2. If $\frac{K_{dr_k}}{K_{dr_2}}$ is sufficiently large, VSC_k can be represented by a constant active power source in the INDSYS model of VSC_2. In the general case, where the droop constants of converters are neither small nor large compared to one another, the adjacent converters operating in droop control mode will be represented by a capacitor and a voltage-dependent power source as shown in the box in Fig. 5b. Table 2 shows the DC side dynamics of INDSYS models shown in Fig. 5. This Table focuses on how the dynamics of adjacent converters must be included in the model of VSC_2.

Table 2
The DC side dynamics of two INDSYS models of VSC_2 in droop control mode.

Model No. 1-Droop	Model No. 2-Droop
	$C_2 \frac{dv_{dc_2}}{dt} = i_{12}^{dc} - \frac{P_2}{v_{dc_2}}$
	$L_L \frac{di_{12}^{dc}}{dt} + R_L i_{12}^{dc} = v_{dc_1} - v_{dc_2}$
	$L_L \frac{di_{13}^{dc}}{dt} + R_L i_{13}^{dc} = v_{dc_1} - v_{dc_3}$
$C_2 \frac{dv_{dc_2}}{dt} = -i_2^{dc_0} - \frac{P_2}{v_{dc_2}}$	$C_1 \frac{dv_{dc_1}}{dt} = -(i_{12}^{dc} + i_{13}^{dc}) - \frac{P_1}{v_{dc_1}}$
	$P_1 = P_{1,0} - \frac{1}{K_{dr_1}}(v_{dc_{1,0}} - v_{dc_1})$
	$C_3 \frac{dv_{dc_3}}{dt} = i_{13}^{dc} - \frac{P_3}{v_{dc_3}}$
	$P_3 = P_{3,0} - \frac{1}{K_{dr_3}}(v_{dc_{3,0}} - v_{dc_3})$

Therefore, the dynamic equation of P_2, which depends on the internal dynamics of VSC_2, is not presented.

If at least one of the converters is in APCM rather than in droop control mode, the INDSYS model of this converter will be model No. 1-APCM shown in Fig. 4a. The impact of this converter on the INDSYS model of other converters that operate in droop control mode will be similar to Fig. 5b, where the droop constant of the converter in APCM is very large compared to the droop constants of other converters.

5. Validation of the INDSYS models

Prior to the comparative study, model validation is performed for model No. 1-DVCM and model No. 2-DVCM proposed in Fig. 3 and model No. 2-Droop in Fig. 5. In this process, the nonlinear electromagnetic transient (EMT) model, built in PSCAD environment, the averaged nonlinear model, built in SIMULINK, and the small-signal (linear) model are compared against each other. The required system and control parameters are given in Table 3. It should be mentioned that the system model built in PSCAD includes a parallel second order RLC filter with f_{cut} = 450 Hz for filtering the switching harmonics. Figs. 6–7 show the response of the models to a 10% change applied to the DC voltage at t = 8 s. The model validation confirms that the small-signal models used in this paper are accurate.

Table 3
Parameters of the test system [26].

Quantity	Value	Description
P	200 MW	Active power
V_{dc}	400 KV	DC voltage
V_s	230 KV	AC grid RMS voltage
f	60	Frequency
L	0.0291 H	Filter inductance
R	0.005 Ω	Filter and switches on-state resistance
C_{dc}	300 μ F	DC side capacitance
τ	2 ms	Inner current loop time constant
K_p^{pll}, K_I^{pll}	30,460	Proportional and integral gains of PLL

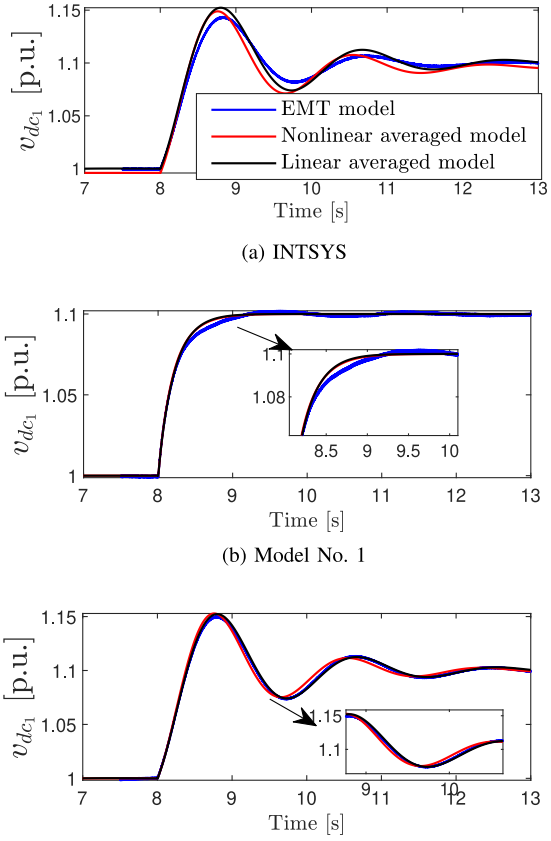

(a) INTSYS

(b) Model No. 1

(c) Model No. 2

Fig. 6. Validation of the models in the master–slave mode of operation: time-domain response of the EMT, nonlinear averaged, and linear averaged models to a 10% change in the DC voltage at t = 8 s.

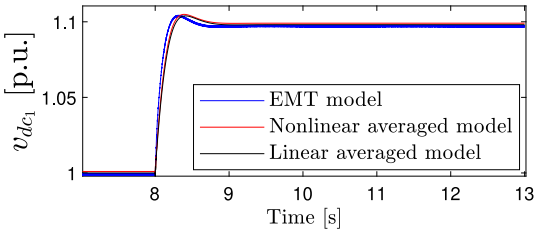

Fig. 7. Validation of model No. 2-Droop in the droop control mode: time-domain response of the EMT, nonlinear averaged, and linear averaged models to a 10% change in the DC voltage at t = 8 s.

6. Comparative study of INDSYS models for the master-slave mode of operation

According to Section 3, for a VSC in APCM, the INDSYS model No. 1-APCM (Fig. 4a) is selected, while for a VSC in DVCM, there are two potential INDSYS models shown in Fig. 3. In this section, the suitable model among these two models will be identified using the eigenvalue, participation factor, and sensitivity analyses. These analyses are used to determine how the stability and dynamic performance of INTSYS are impacted by the type of INDSYS model.

6.1. Eigenvalue analysis

Fig. 8 compares INDSYS model No. 1-DVCM and No. 2-DVCM of VSC_1 shown in Fig. 3 in terms of the closeness of their eigenvalue locus

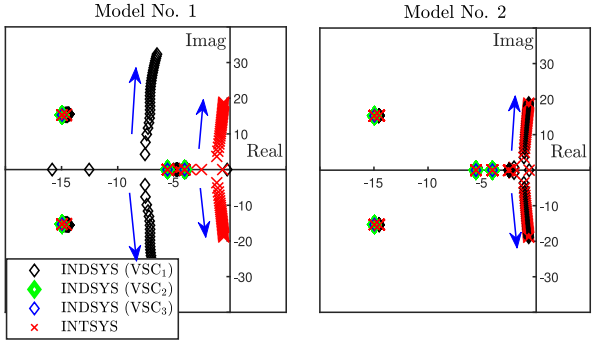

(a) Sweep of K_{I_1}={1;300} and K_{p_1}=2

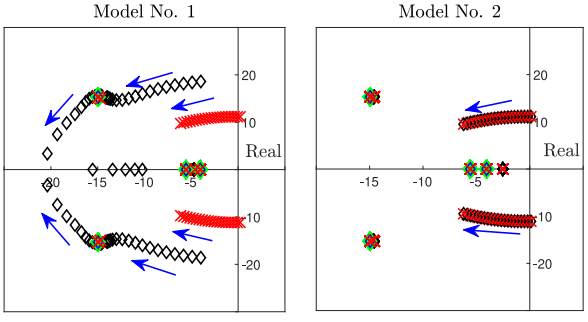

(b) Sweep of K_{p_1}={0.3;10.5} and K_{I_1}=100

Fig. 8. Eigenvalue locus of INDSYS and INTSYS models for SCR = 4 and a sweep of DC voltage controller parameters.

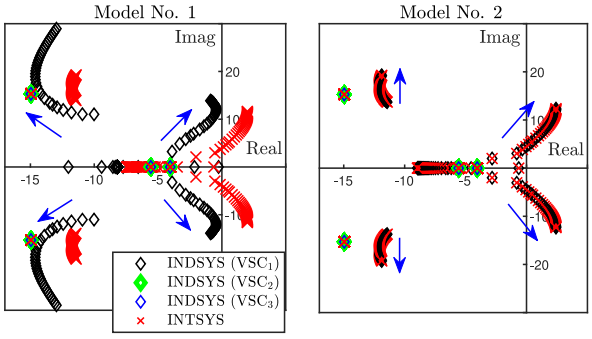

(a) Sweep of K_{I_1}={1;300} and K_{p_1}=2

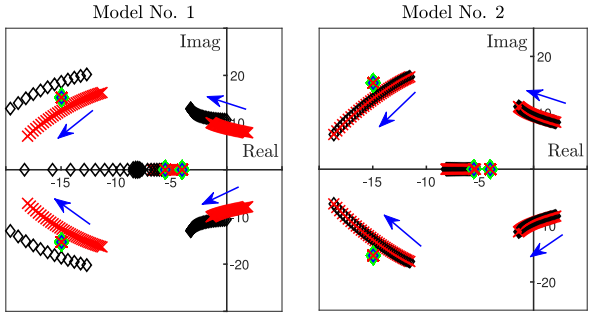

(b) Sweep of K_{p_1}={0.3;18.5} and K_{I_1}=100

Fig. 9. Eigenvalue locus of INDSYS and INTSYS models for SCR = 1.5 and a sweep of DC voltage controller parameters.

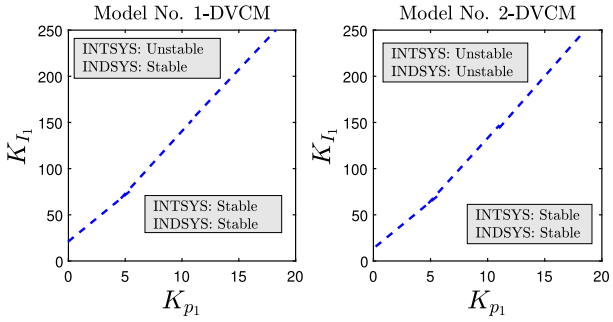

Fig. 10. Stability region of INTSYS vs. stability region of INDSYS models of VSC_1 (SCR = 1.5).

to that of the INTSYS model under changing VSC_1 controller parameters. While the focus is on choosing the suitable INDSYS model for VSC_1 (in the DVCM), the eigenvalues associated with the INDSYS model of all three VSCs are plotted to show the correspondence between the eigenvalues of the INTSYS and the aggregate of the INDSYS models. Fig. 8a and b respectively show the impact of changing the integral gain (K_{I_1}) and the proportional gain (K_{p_1}) of the DC voltage controller on the eigenvalue locus of the INDSYS model of VSC_1 and INTSYS. The q-axis controller of VSC_1 is set to $\frac{16.46}{s}$. According to Fig. 8, the eigenvalue locus of INTSYS and INDSYS models do not match for model No. 1-DVCM. However, employing model No. 2-DVCM leads to an exact matching between the eigenvalues of INTSYS and INDSYS models.

Fig. 9 is the counterpart of Fig. 8 for a low SCR (SCR = 1.5) associated with the AC grid connected to VSC_1. Similar to Figs 8, 9 also shows a deviation in the eigenvalue locus of INTSYS and that of the INDSYS model No. 1-DVCM. Furthermore, Fig. 9 shows that while the INDSYS models are stable, the INTSYS might become unstable with variations of controller parameters. Thus, not only do the eigenvalues

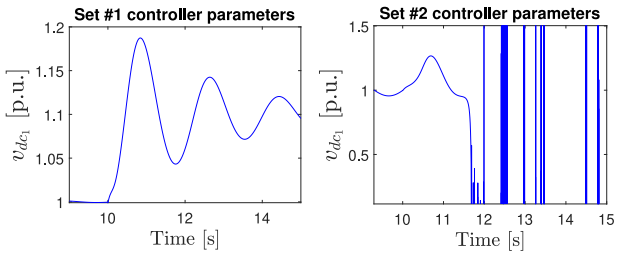

(a) INTSYS

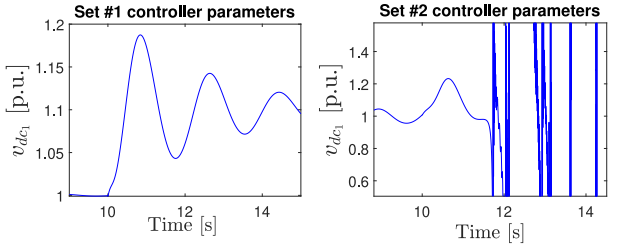

(b) INDSYS model No. 2

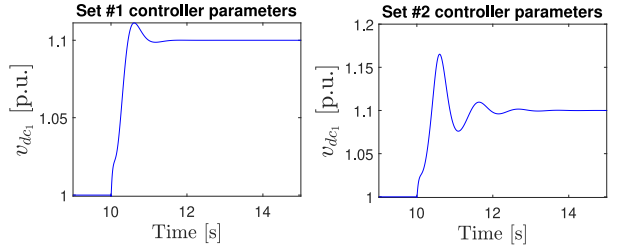

(c) INDSYS model No. 1

Fig. 11. Time-domain response of (a) INTSYS model, (b) INDSYS model No. 2-DVCM, and (c) INDSYS model No. 1-DVCM, to a 10% change in the DC voltage. Controller set 1: $K^o_{d_1} = 2.5 + \frac{10}{s}$, and controller set #2: $K^o_{d_1} = 2.5 + \frac{20}{s}$. $K^o_{q_1} = 0.002 + \frac{11.5}{s}$ for both cases.

of INTSYS deviate from the INDSYS model No. 1-DVCM, but instability occurs in INTSYS for a range of control parameters even though the INDSYS models are stable. Therefore, with these models, no mitigation approach can be taken during the individual design of converter controllers to stabilize the INTSYS as no instability is observed in the INDSYS models. Stabilizing the INTSYS, in this case, would require access to the entire INTSYS model and retuning of the individually designed controllers. Selecting model No. 2-DVCM, however, can solve this issue because whenever the INTSYS is unstable, the INDSYS model is unstable as well. Therefore, the INTSYS can be stabilized via the proper design of individual controllers.

To illustrate the significance of selecting proper models for individual converter controllers' design on the stability of the INTSYS, Fig. 10 compares the stability regions of the INTSYS model and INDSYS model of VSC_1. According to Fig. 10, the allowable range of controller parameters to ensure the INTSYS stability shrinks with the connection of the converters to a shared DC system, and as a result, the INTSYS might lose stability even when VSC_1 is stable. However, the stability regions of the INDSYS model of VSC_1 and INTSYS model are exactly the same when model No. 2-DVCM is selected for designing the controllers of VSC_1.

To verify the conclusion made based on Fig. 10, the time-domain response of the INTSYS and INDSYS models to a small disturbance in the DC voltage for two sets of parameters are depicted in Fig. 11. The parameters of set 1 (corresponding to the stable region of INTSYS) are $K_{p_1} = 2.5, K_{I_1} = 10$, and the parameters of set 2 (corresponding to the

unstable region of INTSYS) are $K_{p_1} = 2.5, K_{I_1} = 20$. Fig. 11 shows that all three models are stable for set 1 parameters. However, only INDSYS model No. 1-DVCM is stable for set 2 parameters. This confirms that the stability region of model No. 1-DVCM is not similar to that of INTSYS, and thus, a controller designed for VSC_1 based on INDSYS model No. 1-DVCM will not stabilize the INTSYS.

6.2. Participation factor analysis

To identify the state variables that contribute significantly to the unstable modes of INTSYS in Fig. 9 and to determine whether model No. 2-DVCM, which showed the same eigenvalues as that of the INTSYS, includes these state variables, participation factor analysis is used. If model No. 2-DVCM includes the corresponding states, a controller designed based on this model for a converter in DVCM will stabilize the INTSYS.

Fig. 12 shows the participation factors of INTSYS state variables in the unstable modes. The state variables of each converter are shown on the horizontal axis, and the vertical axis shows the participation factors. Because Fig. 12 is plotted for the sweep of controller parameters of VSC_1, the state variables associated with the outer controller of VSC_1 are also highlighted on the horizontal axis. The sweep of parameters is similar to that in Fig. 9. It should be mentioned that the state variables and their order are similar to those in (1)–(2). Considering Fig. 12, the highest participation in the unstable modes is associated with the state variables of VSC_1 (in particular i_{dq_1}, v_{dc_1}, and the state variable associated with VSC_1 d-axis outer controller). The DC voltages of VSC_2 and VSC_3 (states number 11 and 21) also impact the unstable modes. Based on the discussion provided in Section 3.2, the DC voltage is not included in the INDSYS model of a converter in APCM. Therefore, to contain all the dynamics causing instability in the INDSYS models,

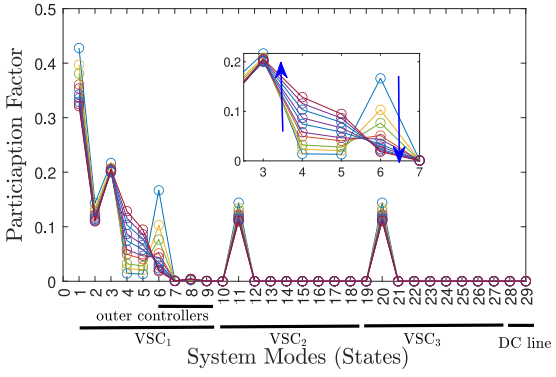

(a) Sweep of K_{I_1}={1;300} and K_{p_1}=2

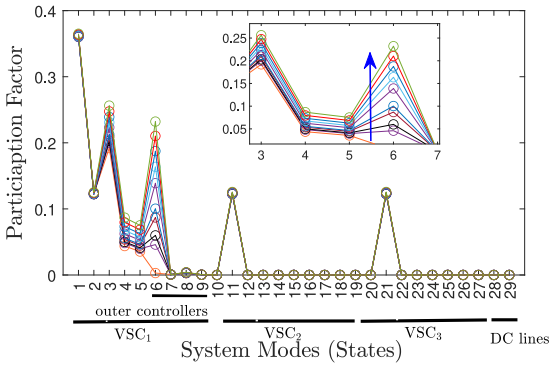

(b) Sweep of K_{p_1}={0.3;18.5} and K_{I_1}=100

Fig. 12. Participation factors for INTSYS system's unstable modes in Fig. 9 with (a) sweep of K_{I_1} and (b) sweep of K_{p_1}.

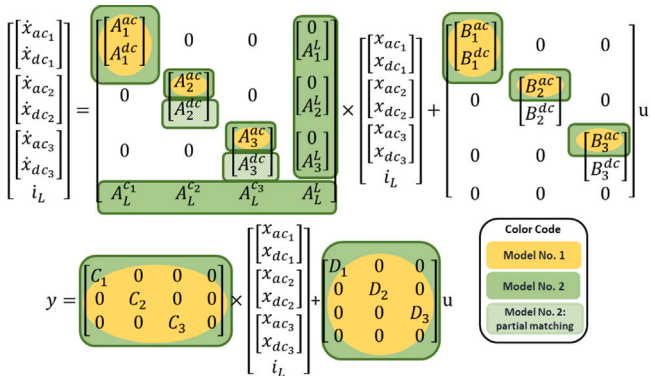

Fig. 13. The matching level between INTSYS and INDSYS state-space models.

the dynamics of capacitors of the converters in APCM (states number 11 and 21) must be considered in the INDSYS model of VSC_1, which operates in DVCM. Referring to Fig. 3, only INDSYS model No. 2-DVCM includes these necessary state variables.

6.3. Sensitivity analysis

According to the eigenvalue and participation factor analyses, model No. 2 for a converter in DVCM provides a close matching between the eigenvalues of the INDSYS and INTSYS models and also includes the required state variables that may cause instability. However, there exist discrepancies between the state-space model of INTSYS, given by (1)–(2), and that of INDSYS, given by (3)–(4) and (6)–(7). Fig. 13 shows the state-space model of the INTSYS in comparison to those of the INDSYS models. Yellow and green colors respectively correspond to INDSYS models No. 1-DVCM and No. 2-DVCM of VSC_1 shown in Fig. 3. The state-space representation of INDSYS models only include the elements that are highlighted in their corresponding color.

Fig. 13 confirms that there is a significant discrepancy between the A matrix of the INTSYS and INDSYS model No. 1-DVCM. Between the two INDSYS models for a converter in DVCM, model No. 2-DVCM (Fig. 3b) shows the largest similarity with the INTSYS. Although there is a significant matching between the state-space representation of the INTSYS and INDSYS model No. 2-DVCM, some discrepancies remain between the two models as the internal dynamics of the converters in APCM are ignored in model No. 2-DVCM. These discrepancies, which correspond to the partial matching or no matching between the dynamics of the INTSYS and model No. 2-DVCM are represented by A_2^{dc}, A_3^{dc}, B_2^{dc}, and B_3^{dc} matrices.

To verify whether this mismatch deteriorates the accuracy of INDSYS model No. 2-DVCM, the sensitivity of eigenvalues of the closed-loop system with respect to the elements of A_2^{dc}, B_2^{dc}, A_3^{dc}, and B_3^{dc} matrices in Fig. 13 is computed as

$$\frac{\partial \lambda_i}{\partial a_{kj}} = \Psi_{ik}\Phi_{ji}, \tag{10}$$

where Ψ_{ik} and Φ_{ji} are the elements of the left and right eigenvectors associated with λ_i [27], and a_{kj} corresponds to the elements of the INTSYS state matrix that are associated with A_2^{dc}, B_2^{dc}, A_3^{dc}, and B_3^{dc} (each of VSC_2 and VSC_3 has five state variables, so a_{kj} has 5 elements per converter). The sensitivity of all the eigenvalues to the elements of matrices corresponding to the mismatches is plotted in Fig. 14, where each color represents one eigenvalue. Fig. 14 illustrates that the sensitivity of eigenvalues to the elements that do not match between the INTSYS and INDSYS state-space models is very small, showing that their inclusion or exclusion in the models does not considerably impact the eigenvalue locus. Therefore, Figs. 3b and 4a provide precise models respectively for a converter in DVCM and for a converter in APCM.

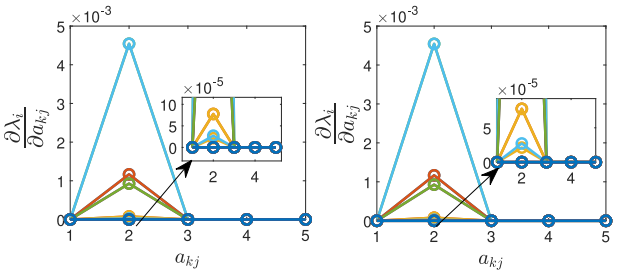

(a) SCR=4

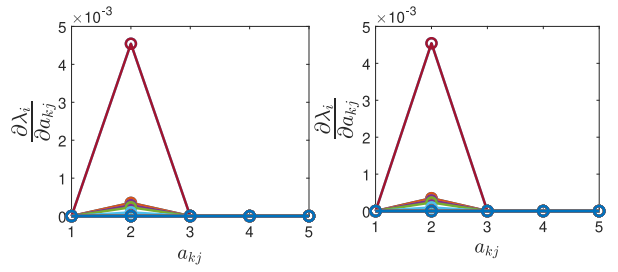

(b) SCR=1.5

Fig. 14. Sensitivity of eigenvalues with respect to a_{kj}: (on the left: a_{kj} associated with A_2^{dc} and B_2^{dc}, and on the right: a_{kj} associated with A_3^{dc} and B_3^{dc}).

7. Comparison of INDSYS models for converters in droop control mode of operation

Several droop constants are presented in Table 4 and are used to specify which one of the INDSYS models in Fig. 5 is a suitable choice for the individual control design of converters.

In set 1, the droop constant of VSC_1 is small, while the two other droop constants are large. Therefore, based on the discussion in Section 4, in the INDSYS model of VSC_1, VSC_2 and VSC_3 can be considered as active power sources. Likewise, in the INDSYS models of VSC_2 and VSC_3, VSC_1 can be considered as a constant voltage source. Fig. 15 shows the eigenvalue locus of INDSYS and INTSYS models for droop set 1. Fig. 15a and b respectively show the eigenvalue locus for the current source model and model No. 2-Droop. The eigenvalue locus of INTSYS and INDSYS models are similar in Fig. 15b, while they are different in Fig. 15a, showing that the current source model is not suitable, but the model of Fig. 5b contains the necessary coupling dynamics. Similar observations were made for droop set 2. Therefore, for droop sets 3 and 4, only model No. 2-Droop (Fig. 5b) will be considered, and its accuracy will be analyzed.

In the third and fourth sets of droop constants in Table 4, the droop constants for all the VSCs are the same. Fig. 16 shows the eigenvalue locus of the INTSYS model and the INDSYS model No. 2-Droop for droop set 3, where each color is associated with one specific set of control parameters. Based on Fig. 16, adjacent to each eigenvalue of the INDSYS there exists an eigenvalue associated with the INTSYS. In some cases, the exact matching between the eigenvalues of INTSYS and INDSYS does not happen, though they remain close to each other. The reason is that model No. 2-Droop does not include the internal dynamics of adjacent VSCs, even though the coupling between the DC

Table 4
Set of droop constants.

	Set 1	Set 2	Set 3	Set 4
Droop constants	$K_{d_1} = 0.1$ $K_{d_2} = 10$ $K_{d_3} = 10$	$K_{d_1} = 10$ $K_{d_2} = 0.1$ $K_{d_3} = 0.1$	$K_{d_1} = 1$ $K_{d_2} = 1$ $K_{d_3} = 1$	$K_{d_1} = 3$ $K_{d_2} = 3$ $K_{d_3} = 3$

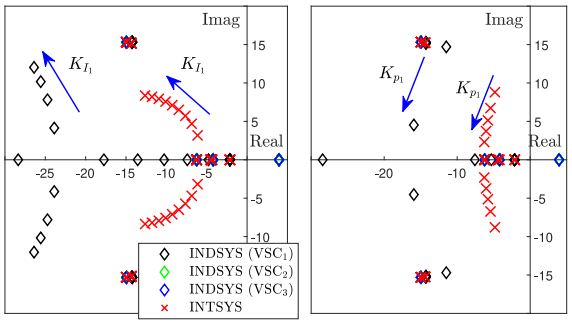

(a) Model No. 1

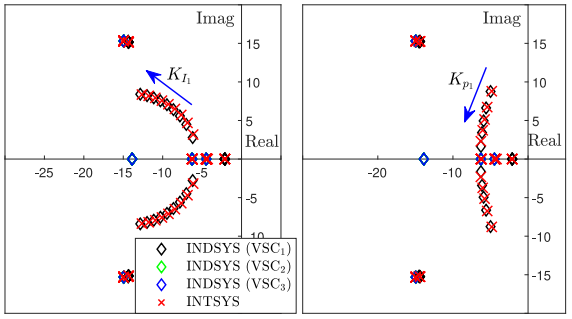

(b) Model No. 2

Fig. 15. Eigenvalue locus of INTSYS and INDSYS models for droop set 1 for (a) model No. 1 and (b) model No. 2, with the sweep of parameters of VSC_1: (on the left: K_{p_1} = {0.3;2.5} and K_{I_1} = 10, and on the right: K_{I_1} = {10;50} and K_{p_1} = 2), and SCR = 4.

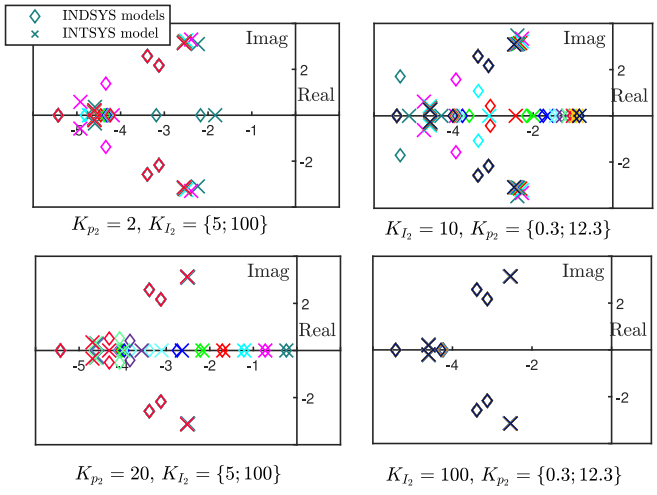

Fig. 16. Eigenvalue locus of INTSYS and INDSYS models (model No. 2-Droop) for a sweep of controller parameters for droop set 3.

voltage and the active power in the droop control mode is incorporated into the INDSYS model. Similar conclusions can be made for droop set 4.

To better compare the eigenvalue locus of INTSYS and INDSYS models, Fig. 17 shows the magnitude and the phase angle of dominant eigenvalues of the two models against control parameters of VSC_2 for droop sets 2–4. Due to the symmetry of the eigenvalue locus with respect to the real axis, the phase angles associated with only one of the complex-conjugate oscillatory modes are shown. Fig. 17a and

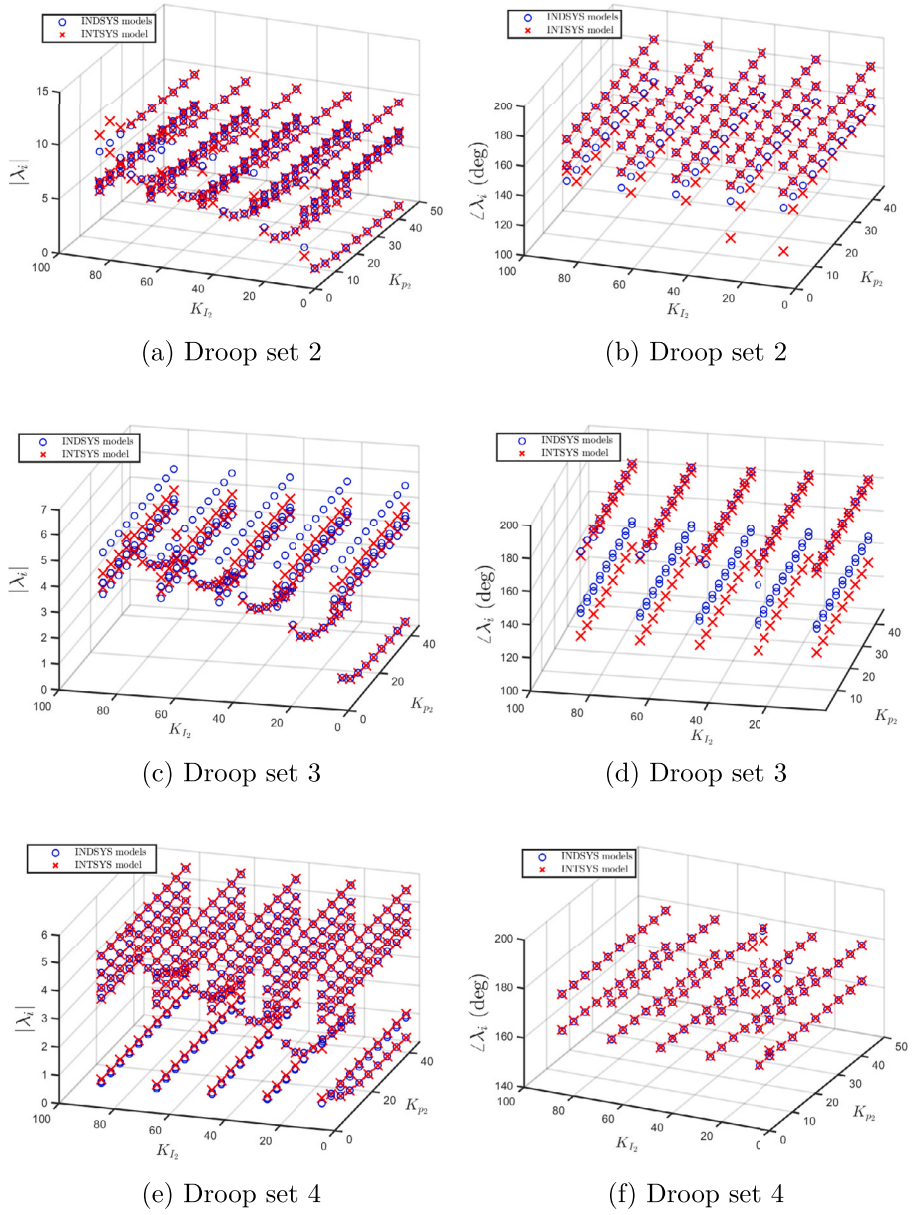

Fig. 17. Magnitude and phase angle of all the eigenvalues close to the imaginary axis against controller parameters for (a-b) droop set 2, and (c-d) droop set 3, and (e-f) droop set 4.

b, associated with droop set 2, show a close matching between the magnitude and phase angle of eigenvalues of the INDSYS and INTSYS, confirming the conclusion made based on Fig. 15. Fig. 17c-d and e-f indicate a close matching between the eigenvalue locus of the INDSYS and INTSYS for equal droop constants and confirm the observations based on Fig. 16. According to Fig. 17e and f, the magnitude and phase angle of eigenvalues of INTSYS and INDSYS models for droop set 4 are closer to each other compared to those depicted in Fig. 17c and d for droop set 3. The reason can be explained based on model No. 2-Droop in Fig. 5b. When the droop constants become larger, $\frac{1}{K_{dr_k}}$ becomes smaller. As a result, according to (9), the adjacent converters that are represented by the voltage-dependent power source in Fig. 5b behave comparable to a constant active power source. In such a case, the coupling between the DC voltage and active power of adjacent converters becomes weaker, and the INDSYS models, which do not include the internal dynamics of adjacent converters, provide a closer match to the INTSYS model in terms of dynamic response.

Due to the coupling among the VSCs in the droop mode of operation, the superimposed eigenvalue of INDSYS models may be slightly different from that of the INTSYS model. The INDSYS model might not be an exact duplicate of INTSYS. However, INDSYS stability ensures INTSYS stability as the eigenvalues are in the same neighborhood. It should be noted that the purpose is to exclude the internal dynamics of adjacent VSCs from the INDSYS models, simplify the stability analysis and design the controllers individually while preventing the INTSYS instability. If the internal dynamics of adjacent VSCs are considered in the models, the control system design cannot be decomposed into that of smaller subsystems.

8. Conclusion

The objective of this paper was to determine the appropriate system models that capture the necessary coupling dynamics among the VSCs for an individual control design of the VSCs embedded in AC-MTDC systems. A controller that is designed individually based on

the appropriate model can be employed in the interconnected system (INTSYS) without causing instability or poorly damped modes. The suitable individual system (INDSYS) models were selected such that they did not include the adjacent VSCs' internal dynamics but included the necessary coupling dynamics to prevent uncontrollable dynamic interactions among converters. Participation factor, sensitivity, and eigenvalue analyses were performed to verify the accuracy of the models.

The studies demonstrated that for a converter in DC voltage control mode, the only model that leads to an exact matching between the eigenvalue locus of INTSYS and INDSYS models was the one that included the dynamics of DC transmission lines and the capacitor of the converters in the active power control mode (APCM). For a converter in APCM, including the converter's AC side dynamics in the INDSYS model was sufficient, and including the DC voltage dynamics was not necessary. For the droop control mode of operation, the model that included the DC transmission line and the operating mode of adjacent converters through a voltage-dependent power source led to the best match between INTSYS and INDSYS models. The impact of AC system SCR on INTSYS stability was also discussed. It was shown that for low SCR values, selecting a suitable INDSYS model for control design is important, because the individually designed converter controllers may not stabilize the INTSYS.

CRediT authorship contribution statement

Fatemeh Ahmadloo: Conceptualization, Methodology, Software, Formal analysis, Validation, Investigation, Resources, Writing – original draft. **Sahar Pirooz Azad:** Visualization, Supervision, Project administration, Writing – review & editing.

Declaration of competing interest

There is no conflict of interests.

Data availability

No data was used for the research described in the article.

References

[1] Van Hertem D, Ghandhari M. Multi-terminal VSC HVDC for the European supergrid: Obstacles. Renew Sustain Energy Rev 2010;14(9):3156–63.
[2] Beerten J, D'Arco S, Suul JA. Identification and small-signal analysis of interaction modes in VSC MTDC systems. IEEE Trans Power Deliv 2015;31(2):888–97.
[3] Li G, Du Z, An T, Xia Y, Lei J. Impact of PLL and VSC control parameters on the AC/MTDC systems stability. Electr Power Syst Res 2016;141:476–86.
[4] Yuan Z, Zhengchun D, Li G. Analysis on the dynamic behaviours and interactions of VSC-MTDC grid. IET Gener Transm Distrib 2018;12(8):1756–64.
[5] Fu Q, Du W, Wang H, Ren B, Xiao X. Small-signal stability analysis of a VSC-MTDC system for investigating DC voltage oscillation. IEEE Trans Power Syst 2021.
[6] Li Y, Li J, Xiao H, Zhang J, Du Z. Stability analysis of droop-based converter using SISO method from DC side perturbation. IEEE Trans Power Deliv 2020;36(5):3150–61.
[7] Du W, Fu Q, Wang H. Small-signal stability of an AC/MTDC power system as affected by open-loop modal coupling between the VSCs. IEEE Trans Power Syst 2017;33(3):3143–52.
[8] D'Arco S, Beerten J, Suul J. Classification and analysis of impact on small-signal dynamics and stability from expansion of VSC-HVDC systems to multi-terminal HVDC grids. In: 13th IET international conference on AC and DC power transmission (ACDC 2017). IET; 2017, p. 1–8.
[9] Pinares G, Bongiorno M. Modeling and analysis of VSC-based HVDC systems for DC network stability studies. IEEE Trans Power Deliv 2015;31(2):848–56.
[10] Yogarathinam A, Chaudhuri NR. Stability-constrained adaptive droop for power sharing in AC-MTDC grids. IEEE Trans Power Syst 2019;34(3):1955–65.
[11] Agbemuko AJ, Domínguez-García JL, Prieto-Araujo E, Gomis-Bellmunt O. Advanced impedance-based control design for decoupling multi-vendor converter HVDC grids. IEEE Trans Power Deliv 2020;35(5):2459–70.
[12] Agbemuko AJ, Domínguez-García JL, Gomis-Bellmunt O. Robust decentralized approach to interaction mitigation in VSC-HVDC grids through impedance minimization. Control Eng Pract 2022;118:104346.
[13] Arunprasanth S, Annakkage UD, Karawita C, Kuffel R. Generalized frequency-domain controller tuning procedure for VSC systems. IEEE Trans Power Deliv 2015;31(2):732–42.
[14] Wang W, Beddard A, Barnes M, Marjanovic O. Analysis of active power control for VSC–HVDC. IEEE Trans Power Deliv 2014;29(4):1978–88.
[15] Shen L, Barnes M, Preece R, Milanovic JV, Bell K, Belivanis M. The effect of VSC-HVDC control on AC system electromechanical oscillations and DC system dynamics. IEEE Trans Power Deliv 2015;31(3):1085–95.
[16] Prieto-Araujo E, Egea-Alvarez A, Fekriasl S, Gomis-Bellmunt O. DC voltage droop control design for multiterminal HVDC systems considering AC and DC grid dynamics. IEEE Trans Power Deliv 2015;31(2):575–85.
[17] Sanchez S, Garces A, Bergna-Diaz G, Tedeschi E. Dynamics and stability of meshed multiterminal hvdc networks. IEEE Trans Power Syst 2018;34(3):1824–33.
[18] Wang Y, Wen W, Wang C, Liu H, Zhan X, Xiao X. Adaptive voltage droop method of multiterminal VSC-HVDC systems for DC voltage deviation and power sharing. IEEE Trans Power Deliv 2018;34(1):169–76.
[19] Pedra J, Sainz L, Monjo L. Three-port small signal admittance-based model of VSCs for studies of multi-terminal HVDC hybrid AC/DC transmission grids. IEEE Trans Power Syst 2020;36(1):732–43.
[20] Liu Y, Xie S, Liang H, Cui H. Coordinated control strategy of multi-terminal VSC-HVDC system considering frequency stability and power sharing. IET Gener Transm Distrib 2019;13(22):5188–96.
[21] Li Y, Tang G, Ge J, He Z, Pang H, Yang J, Wu Y. Modeling and damping control of modular multilevel converter based DC grid. IEEE Trans Power Syst 2017;33(1):723–35.
[22] Eriksson R. Current sharing in multiterminal DC grids—The analytical approach. IEEE Trans Power Syst 2018;33(6):6278–88.
[23] Freytes J, Gruson F, Colas F, Rault P, Saad H, Guillaud X. Simplified model of droop-controlled MTDC grid-influence of MMC energy management on DC system dynamics. In: 2018 power systems computation conference. PSCC, IEEE; 2018, p. 1–7.
[24] Cole S, Beerten J, Belmans R. Generalized dynamic VSC MTDC model for power system stability studies. IEEE Trans Power Syst 2010;25(3):1655–62.
[25] Yazdani A, Iravani R. Voltage-sourced converters in power systems: Modeling, control, and applications. John Wiley & Sons; 2010.
[26] 3-terminal HVDC link with 2-level VSC terminals. https://www.pscad.com/knowledge-base/article/191.
[27] Kundur P. Power system stability. Power Syst Stab Control 2007;10.